Polyhedron xxx (xxxx) xxx

Contents lists available at ScienceDirect

Polyhedron

journal homepage: www.elsevier.com/locate/poly

Synthesis, structure and properties of new heterometallic octanuclear $Li_2Na_2Cu_4$ and decanuclear Li_2Zn_8 complexes

Shobhraj Haldar [a], Nityananda Dutta [a], Gonela Vijaykumar [b], Arpan Das [b], Luca Carrella [c], Allen Oliver [d], Manindranath Bera [a,*]

[a] Department of Chemistry, University of Kalyani, Kalyani, West Bengal 741235, India
[b] Department of Chemical Sciences, Indian Institute of Science Education & Research Kolkata, Mohanpur, West Bengal 741246, India
[c] Institut fur Anorganische Chemie und Analytische Chemie, Johannes-Gutenberg Universität Mainz, Duesbergweg 10-14, D-55128 Mainz, Germany
[d] Department of Chemistry and Biochemistry, University of Notre Dame, 251 Nieuwland Science Hall, Notre Dame, IN 46556-5670, USA

ARTICLE INFO

Article history:
Received 2 January 2019
Accepted 9 March 2019
Available online xxxx

Keywords:
Hetero-multimetallic complex
Carboxylate bridging
Crystal structure
Magnetic properties
Thermal behavior

ABSTRACT

A carboxylate containing polydentate ligand in combination with exogeneous succinate (suc) has been used to stabilize heterometallic octanuclear $[Li_2Na_2Cu_4(cpdp)_2(suc)_2(CH_3OH)_2(H_2O)_4]Cl_2{\cdot}6H_2O$ (**1**) and decanuclear $Na(H_3O)_2[Li_2Zn_8(cpdp)_4(suc)_2(H_2O)_4]Cl_2Br_2{\cdot}6MeOH{\cdot}19H_2O$ (**2**) complexes. The reaction of ligand H_3cpdp (H_3cpdp = *N,N'*-bis[2-carboxybenzomethyl]-*N,N'*-bis[2-pyridylmethyl]-1,3-diamino-propan-2-ol) with stoichiometric amounts of $CuCl_2$/sodium succinate, and $ZnCl_2$/sodium succinate, allowed isolation of complexes **1** and **2**, respectively. Analyses of single crystal X-ray structures indicate that complex **1** is capped by two $[Cu_2(cpdp)]^+$ molecular building units and two succinate linkers, while complex **2** is overlaid by four $[Zn_2(cpdp)]^+$ molecular building units and two succinate linkers. Whereas complex **1** shows monodentate terminal and tridentate $\mu_3{:}\eta^2{:}\eta^1{:}\eta^1$ bridging coordination of carboxylate, and $\mu_4{:}\eta^2{:}\eta^1{:}\eta^1{:}\eta^1$ bridging mode of succinate, complex **2** displays monodentate terminal and anti-anti $\mu_2{:}\eta^1{:}\eta^1$ bidentate bridging coordination of carboxylate, and $\mu_4{:}\eta^1{:}\eta^1{:}\eta^1{:}\eta^1$ bridging mode of succinate. To our knowledge, **1** is the first example of copper/lithium/sodium-based hetero-octanuclear complex with any class of bridging or non-bridging ligand showing three different binding modes of carboxylates. Again, **2** is also the first example of a hetero-decanuclear metallomacrocyclic complex with any class of bridging or non-bridging ligand combining both lithium and zinc. Variable temperature magnetic investigation of **1** discloses sensible antiferromagnetic interactions intermediated among the copper centers. Thermal behavior of **1** and **2** has been examined by thermogravimetric analysis indicating that the complexes are stable up to ~430 °C.

1. Introduction

In recent years, the study of multinuclear complexes of metals in moderate oxidation states has become one of intense research interest not only because of their attractive and diverse multidimensional architectures, but also due to their many applications, including magnetic properties [1–7]. Some examples with fascinating magnetic properties include single molecule magnets [8–11] or magnetic refrigerants [12] and molecules with large spin ground states [13] or large anisotropy barriers [14]. In multinuclear complexes, the neighboring metal centers are likely to cooperate in promoting reactions which have frequently been observed in biological systems. Many multinuclear protein complexes that carry out an extraordinary array of catalytic transformations have been created by nature [15–18]. To comprehend and exploit such phenomena, additional examples of high nuclearity homo- and heterometallic complexes are required, and this is a challenge to the synthetic chemists. In contrast to the homometallic multinuclear complexes, the assembly of heterometallic multinuclear complexes containing both transition and alkali metals has been largely unexplored. Therefore, the search for appropriate organic ligands to bridge the gap between transition and alkali metals is an attractive but highly challenging task since these heterometallic multinuclear complexes should provide the chance to produce multifunctional materials. In this line, the presence of alkali metal ions in the reaction system sometimes assist the assembling process for construction of heterometallic multinuclear complexes [19,20]. Therefore, the introduction of alkali metal Li/Na/K cations into the metal-carboxylate frameworks is interesting for many

* Corresponding author.
E-mail address: mbera2009@klyuniv.ac.in (M. Bera).

https://doi.org/10.1016/j.poly.2019.03.013
0277-5387/

potential applications as well as in directing the formation of multinuclear complexes with diverse and aesthetically pleasant structural design. On the other hand, succinate (suc) being a linear dicarboxylate exhibiting multidimensional metal–oxygen connectivity in their complexes, provides an effective means for the synthesis of multinuclear complexes with novel topologies and other properties [21,22].

Careful literature search also shows that succinate has been little employed as bridging ligand in the synthesis of heterometallic multinuclear complexes; only very few high nuclearity ($N \geq 6$) transition metal complexes are structurally characterized [23,24]. Therefore, yielding these heterometallic complexes by using two, or more, different metal ions is a smart synthetic target. However, in spite of great synthetic challenge, there are significant potential rewards with real possibility of control/design over the discrete magnetic parameters that add to their overall molecular properties [25]. In this field, we have explored the feasibility of carboxylate-based polydentate ligands in presence of different exogeneous bridging groups to influence the nuclearity and topology of multinuclear complexes [26–28]. We have since observed the modification of ligands and reaction conditions to allow access to different multinuclear complexes, the assembly of which can be understood in terms of bridging potential of different endo- and exogeneous functionalities. This article discusses the simple and facile approach to synthesize succinate incorporated, two novel heterometallic, an octanuclear $Li_2Na_2Cu_4$ and a decanuclear Li_2Zn_8 complexes of a polydentate ligand showing rare and interesting coordination chemistry. Additionally, structural aspects, magnetic and thermal behavior have been discussed.

2. Experimental

2.1. Reagents and solvents

2-Carboxybenzaldehyde, 2-picolylchloride hydrochloride, 1,3-diamino-2-propanol, sodium borohydride and lithium hydroxide were purchased from Sigma-Aldrich Chemie GmbH, Germany and were used as received. Copper(II) chloride dihydrate, zinc(II) chloride and sodium succinate hexahydrate were purchased from Merck, India. All other chemicals and solvents were reagent grade materials and were used as received without further purification.

2.2. Physical measurements

Microanalyses analyses of the ligand as well as complexes were carried out by a Perkin-Elmer 2400 Series II elemental analyzer. FTIR spectra were recorded as KBr pellets on a Perkin-Elmer L120-000A spectrometer operating at 400–4000 cm^{-1}. UV–Vis spectra were recorded at room temperature using a UV 1800 (200–900 nm) (1 cm quartz cell) spectrophotometer. ^1H and ^{13}C NMR spectra were obtained on a Bruker AC 400 NMR spectrometer. Mass spectra of the ligand was obtained using a Micromass Q-Tof Micro™ (Waters) mass spectrometer. The potentiometric titration of the ligand H_3cpdp was performed with a Mettler Toledo Seven Compact S220 digital Ion/pH meter using $AgNO_3$ in aqueous solution. The percentage of chloride and bromide present in the ligand were confirmed by potentiometric titration experiment. Thermogravimetric analyses (TGA) were performed with a NETZSCH STA 449F3 thermal analyzer. The XRD measurements were carried out with a Rigaku (Mini Flex II, Japan) powder X-ray diffractometer having Cu Kα = 1.54059 Å radiation. Porosity measurements of **1** and **2** were performed using a Bel Sorp-max instrument from Bel Japan. The variable temperature magnetic susceptibilities of powdered microcrystalline samples of complex **1** were measured using a SQUID magnetometer (MPMS-7, Quantum Design) in the temperature range of 2–300 K under an applied field of 1 Tesla. Experimental susceptibility data were corrected for the underlying diamagnetism using Pascal's constant [29]. The temperature dependent magnetic contribution of the holder was determined experimentally and subtracted from the measured susceptibility data. The program phi [30] was used for spin Hamiltonian simulations of the data.

2.3. Synthesis of N,N′-bis[2-carboxybenzomethyl]-N,N′-bis[2-pyridylmethyl]-1,3-diaminopropan-2-ol, H_3cpdp

The ligand H_3cpdp used in this work was prepared following our previously published procedure [31]. The elemental and thermogravimetric analyses confirmed the composition of the ligand as **H_3cpdp·LiCl·3LiBr·14H_2O**. Yield: 4.018 g (77%). *Anal.* Calc. for $C_{31}H_{32}N_4O_5$·LiCl·3LiBr·14H_2O: C, 33.98%; H, 5.51%; N, 5.11%; Cl, 3.24%; Br, 21.88%. Found: C, 33.88%; H, 5.54%; N, 5.27%; Cl, 2.91%; Br, 21.49%. FTIR (cm^{-1}): ν = 3389(b), 2084(b), 1634(s), 1567(vs), 1441(s), 1399(s), 1298(s), 1154(s), 1094(s), 972(s), 761(s). ^1H NMR (400 MHz, D_2O, room temperature, δ): 8.47 (d, 2H), 7.81 (t, 2H), 7.64 (d, 2H), 7.39–7.51 (m, 8H), 7.27 (d, 2H), 4.47 (d, 8H), 4.01–4.20 (m, 1H), 3.38 (d, 2H), 3.13 (t, 2H). ^{13}C NMR (100 MHz, D_2O, room temperature, δ): 174.65, 149.32, 148.91, 143.99, 141.31, 138.87, 137.23, 133.20, 130.88, 130.44, 125.01, 124.68, 60.47, 60.25, 57.50, 57.11. Mass spectrum (ESI): m/z 565 (100%) (M^+ = {H_3cpdp·H_2O + Li}$^+$), 559 (81%) (M^+ = {H_3cpdp·H_2O + H}$^+$). TGA analysis: loss of H_2O {136–273 °C: 23.00% (Calcd.); 23.35% (Found)}; loss of CO_2 {290–367 °C: 8.03% (Calcd.); 8.39% (Found)}.

2.4. Synthesis of $[Li_2Na_2Cu_4(cpdp)_2(suc)_2(CH_3OH)_2(H_2O)_4]Cl_2$·6$H_2O$ (**1**)

A methanol solution (10 mL) of $CuCl_2$·2H_2O (0.157 g, 0.92 mmol) was added to a solution of H_3cpdp·LiCl·3LiBr·14H_2O (0.511 g, 0.46 mmol) and NaOH (0.055 g, 1.38 mmol) in methanol (10 mL). The reaction mixture was stirred for 1 h at room temperature resulting in a light green solution. Then, an aqueous solution (5 mL) of sodium succinate hexahydrate (0.124 g, 0.46 mmol) was added to this solution and the stirring was continued for another 1 h. Then, the solution became turbid with blue in colour. To remove any insoluble precipitate, the solution was filtered. After one week, blue needle-shaped crystals suitable for X-ray diffraction were obtained by slow diethyl ether diffusion into the clear filtrate at room temperature. Yield: 0.350 g (78%). *Anal.* Calc. for $C_{72}H_{94}N_8O_{30}Cl_2Li_2Na_2Cu_4$ C, 44.66; H, 4.89; N, 5.79; Cu, 13.13. Found: C, 44.27; H, 4.92; N, 5.83; Cu, 13.11. FTIR (cm^{-1}): ν = 3419(b), 2947(b), 1609(s), 1589(s), 1580(s), 1563(s), 1459(s), 1403(s), 1301(s), 1285(s), 1244(s), 1211(s), 1154(s), 1100(s), 1074(s), 1050(s), 1029(s), 996(s), 860(s), 827(s), 763(s), 715(s), 673(s), 524(s). UV–Vis spectra (MeOH): λ_{max} (ε, $M^{-1}cm^{-1}$) = 693 (460), 259 (64956).

2.5. Synthesis of $Na(H_3O)_2[Li_2Zn_8(cpdp)_4(suc)_2(H_2O)_4]Cl_2Br_3$·6MeOH·19$H_2O$ (**2**)

A methanol solution (10 mL) of $ZnCl_2$ (0.125 g, 0.92 mmol) was added to a solution of H_3cpdp·LiCl·3LiBr·14H_2O (0.511 g, 0.46 mmol) and NaOH (0.055 g, 1.38 mmol) in methanol (10 mL). The reaction mixture was refluxed for 1 h, resulting in a light yellow solution. Then, an aqueous solution (5 mL) of sodium succinate hexahydrate (0.124 g, 0.46 mmol) was added to this solution and the mixture was refluxed for another 1 h. Then, the light yellow solution was cooled and filtered. Slow diethyl ether diffusion into the clear filtrate at room temperature produced light yellow block-shaped single crystals suitable for X-ray diffraction after 5–7 days. Yield: 0.365 g (82%). *Anal.* Calc. for $C_{138}H_{200}N_{16}O_{59}Cl_2Br_3Li_2$-

Please cite this article as: S. Haldar, N. Dutta, G. Vijaykumar et al., Synthesis, structure and properties of new heterometallic octanuclear $Li_2Na_2Cu_4$ and decanuclear Li_2Zn_8 complexes, Polyhedron, https://doi.org/10.1016/j.poly.2019.03.013

$NaZn_8$: C, 42.52; H, 5.17; N, 5.75; Zn, 13.42. Found: C, 42.59; H, 5.08; N, 5.61; Zn, 13.35. FTIR (cm^{-1}): ν = 3424(b), 2922(b), 1608 (s), 1595(s),1588(s), 1571(s), 1483(s), 1447(s), 1430(s), 1394(s), 1299(s), 1247(s), 1159(s),1108(s), 1057(s), 1032(s), 944(s), 894 (s), 870(s), 829(s), 770(s), 722(s), 618(s). ^{1}H NMR (400 MHz, CD_3-OD, room temperature): δ (ppm) = 3.09 (t, 8H, succinate), 3.12–4.24 (m, 52H, aliphatic), 6.72–7.64 (m, 64H, aromatic). ^{13}C NMR (100 MHz, CD_3OD, room temperature): δ (ppm) = 54.82 (4C, CH_2, succinate), 55.07 (8C, CH_2), 61.81 (8C, CH_2), 63.69 (8C, CH_2), 63.80 (4C, aliphatic CH), 122.89 (8C, aromatic CH), 123.00 (8C, aromatic CH), 128.32 (8C, aromatic CH), 128.95 (8C, aromatic CH), 129.14 (8C, aromatic CH), 131.38 (8C, aromatic CH), 131.58 (8C, aromatic CH), 139.61 (8C, aromatic CH), 139.79 (8C, aromatic CH), 146.78 (8C, aromatic CH), 157.05 (8C, aromatic CH), 176.11 (4C, monodentate terminal carboxylate, aromatic), 176.22 (4C, bidentate bridging carboxylate, aromatic), 180.70 (4C, bidentate bridging carboxylate, succinate), 180.91 (4C, bidentate bridging carboxylate, succinate). UV–Vis spectra (MeOH): λ_{max} (ε, M^{-1} cm^{-1}) = 264 (50518).

2.6. X-ray crystal structure determination and refinement

The single crystal X-ray data for **1** were collected on a diffractometer with Bruker SMART CCD area detector using a graphite-monochromated Mo Kα radiation (λ = 0.71073 Å) and the data for **2** were collected on a diffractometer with SuperNova, Dual, Cu at zero, Eos area detector [32,33], using a graphite-monochromated Mo Kα radiation (λ = 0.71073 Å). The statistical tests were used to determine the triclinic space group $P\bar{1}$ for both **1** and **2**. A total of 9768 data were measured with Miller indices h_{min} = −15, h_{max} = 15, k_{min} = −18, k_{max} = 18, l_{min} = −18, l_{max} = 18, in the range of 3.014 < θ < 27.553° for **1**, and a total of 19 241 data were measured with Miller indices h_{min} = −17, h_{max} = 17, k_{min} = −23, k_{max} = 22, l_{min} = −24, l_{max} = 24, in the range of 1.7241 < θ < 28.0495° for **2**, using ω oscillation frames. The data were corrected for absorption by the multi-scan method [34] giving minimum and maximum transmission factors. The structures of both **1** and **2** were solved by direct methods using the software SIR-97 [35], and refined by full-matrix least-squares methods against F^2 with the programs SHELXL [36,37] embedded in the routine Olex2 [38]. The residual electron densities in **1** and **2** were in the range of −1.163 to 2.009 e·Å^{-3} and +1.359 to −0.716 e·Å^{-3}, respectively. The difference Fourier map was used to locate the hydrogen atoms. The hydrogen atoms were fixed at ideal positions and refined as riding models.

3. Results and discussion

3.1. Synthesis and general characterization

The ligand adopted for the aforesaid work is H_3cpdp (Scheme 1) [31], which was recently used in our laboratory to build PO_4^{3-}/HPO_4^{2-}, AsO_4^{3-}/$HAsO_4^{2-}$, phthalate/terephthalate and OH^--bridged iron(III), copper(II) and zinc(II) multinuclear complexes [26,39–41]. Very recently, it was also utilized for the construction of a CO_3^{2-} incorporated staircase-like decanuclear copper(II) complex [28]. In fact, room temperature reaction among H_3cpdp, $CuCl_2$ and sodium succinate in a 1:2:1 molar ratio, respectively, in MeOH/H_2O (4:1; v/v) in the presence of NaOH afforded a blue heterometallic octanuclear complex, $[Li_2Na_2Cu_4(cpdp)_2(suc)_2(CH_3OH)_2(H_2O)_4]Cl_2{\cdot}6H_2O$ (**1**) (Scheme 2). However, the pale yellow heterometallic decanuclear complex, $Na(H_3O)_2[Li_2Zn_8(cpdp)_4(suc)_2(H_2O)_4]Cl_2Br_3{\cdot}6MeOH{\cdot}19H_2O$ (**2**) (Scheme 2) was produced by reaction of H_3cpdp with $ZnCl_2$ and sodium succinate in a 2:4:1 molar ratio, respectively, in MeOH/H_2O (4:1; v/v) in the presence of NaOH under refluxing conditions. Elemental analysis, FTIR, UV–Vis, ^{1}H and ^{13}C NMR spectroscopic techniques, TGA analysis, magnetic measurement, and single crystal X-ray method were employed to characterize complexes **1** and **2**. The composition of **1** and **2** was established by elemental and thermal analyses and single crystal X-ray diffraction study.

3.2. Description of the X-ray crystal structure of *1*

Complex **1** crystallized in the triclinic system and the structure was solved in $P\bar{1}$ space group. The asymmetric unit of crystal structure of **1** (Fig. S1, Supplementary Information) contains one lithium(I), one sodium(I) and two copper(II) ions, one $cpdp^{3-}$ and one succinate ligand, and one coordinated methanol and two coordinated water molecules. Two chloride ions as counter anions and six lattice waters are also present in the asymmetric unit. The full structure is generated by growing the asymmetric unit through center of inversion. A view of the crystal structure of hetero-octanuclear unit of **1** is illustrated in Fig. 1. It consists of an octanuclear core in which a cyclic $[Li_2Na_2]$ central unit is linked to two dinuclear $[Cu_2]$ complexes by endogeneous carboxylate and exogeneous succinate bridges. Two carboxylate groups of two $cpdp^{3-}$ ligands exhibit a rare μ_3:η^2:η^1:η^1 tridentate bridging mode (a monodentate and an *anti-anti* bidentate bridge) (Chart 1), with each bridging among one copper, one lithium and one sodium ion. This type of tridentate bridges in metal-carboxylate chemistry is

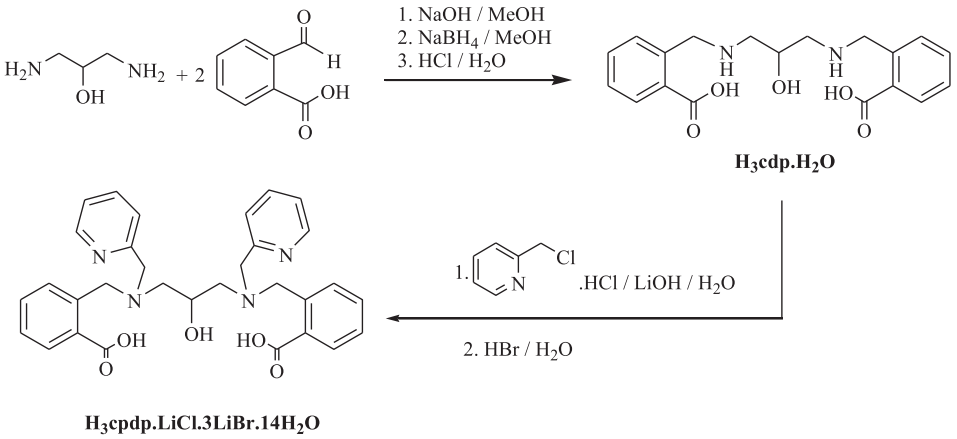

Scheme 1. Synthetic pathway of ligand H_3cpdp.

Please cite this article as: S. Haldar, N. Dutta, G. Vijaykumar et al., Synthesis, structure and properties of new heterometallic octanuclear $Li_2Na_2Cu_4$ and decanuclear Li_2Zn_8 complexes, Polyhedron, https://doi.org/10.1016/j.poly.2019.03.013

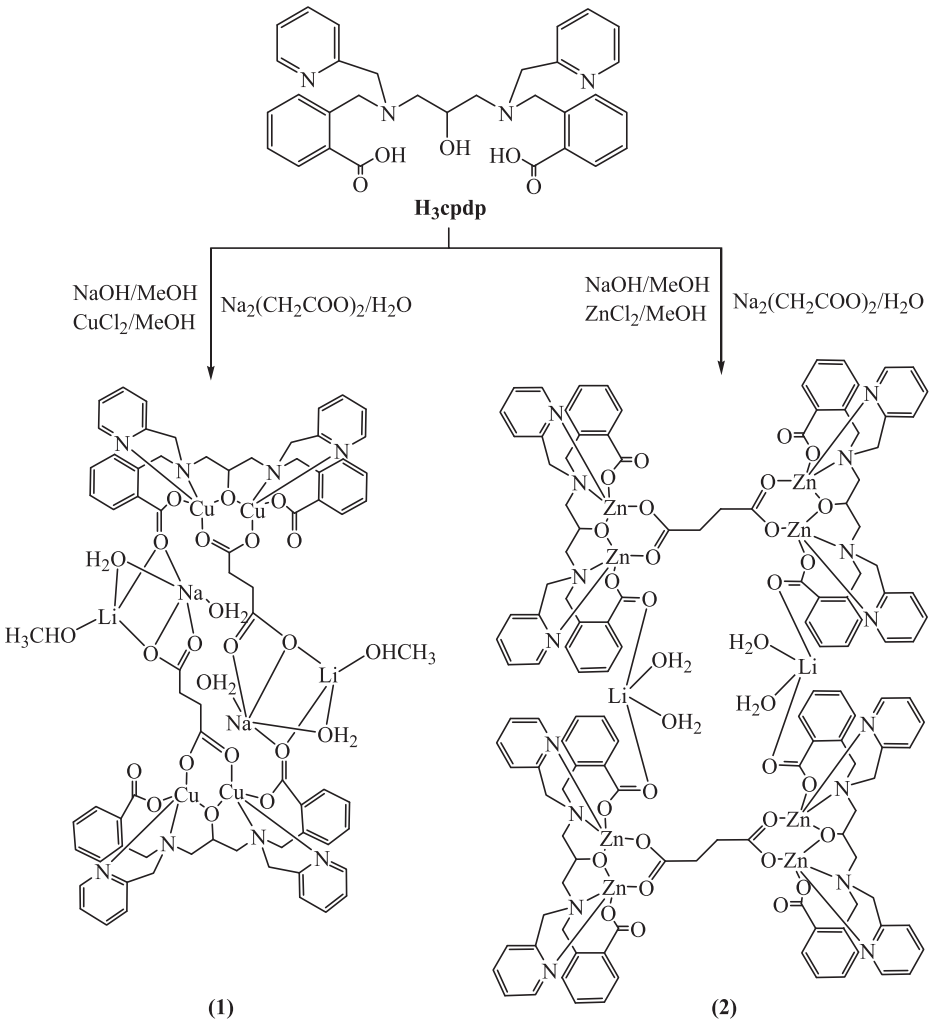

Scheme 2. Synthetic pathway of complexes **1** and **2**.

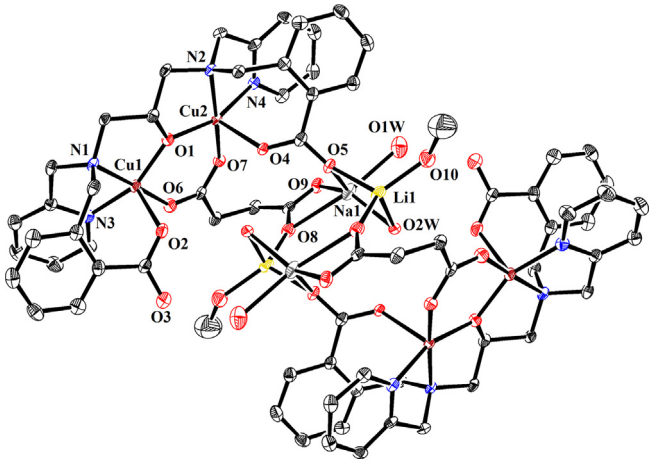

Fig. 1. X-ray crystal structure of **1** with atom numbering scheme. Hydrogen atoms are omitted for clarity.

uncommon [42]. The two independent succinate ligands utilize all four coordinating groups showing an unprecedented μ_4:η^2:η^1:η^1:η^1 bridging mode (Chart 1) linking two copper, one lithium and one sodium ion. Although the μ_4:η^1:η^1:η^1:η^1 bridging mode of succinate is quite common in the literature, the μ_4:η^2:η^1:η^1:η^1 bridging mode is rare [43]. It is fascinating to mention that an eleven membered metallomacrocyclic ring defined by Cu(2)–O(7)–C(32)–C(33)–C(34)–C(35)–O(9)–Na(1)–O(5)–C(31)–O(4) is formed on either side of the [Li_2Na_2] core (Fig. 2).

The coordination sites at the copper centers are occupied by two N-donors provided by one tertiary amine and one pyridyl amine group, and three O-donors provided by one bridging alkoxide, one terminal carboxylate and one bridging succinate group. Geometric constraints imposed by the succinate ligands lead to a distorted square pyramidal (τ = 0.290 for Cu1 and τ = 0.205 for Cu2) [44] copper coordination environments. The deviations of the copper centers from the basal planes are 0.164 (Cu1) and 0.193 Å (Cu2). The coordination environment of lithium(I) ion may be defined by the distorted tetrahedral geometry, with one succinate oxygen, one carboxylate oxygen, one water oxygen and one methanol oxygen atom. On the other hand, the coordination environment of sodium(I) ion may be best described by the distorted trigonal bipyramidal geometry, with two succinate oxygen, one carboxylate oxygen and two water oxygen atoms. The Cu–$O_{alkoxide}$ and Cu–$O_{carboxylate}$ bond distances range from 1.896(3) to 2.214(4) Å, and Cu–N_{amine} bond distances range from 1.986(4) to 2.033(4) Å. [31,41] The intra-metallic separation between the copper centers bridged across the alkoxide group is 3.447(5) Å. Noteworthy here is that the X-ray structure of **1** features carboxylate/water/methanol susceptible hydrogen bonding interactions that contribute towards the stabilization of the crystal lattice (Fig. 3).

Please cite this article as: S. Haldar, N. Dutta, G. Vijaykumar et al., Synthesis, structure and properties of new heterometallic octanuclear $Li_2Na_2Cu_4$ and decanuclear Li_2Zn_8 complexes, Polyhedron, https://doi.org/10.1016/j.poly.2019.03.013

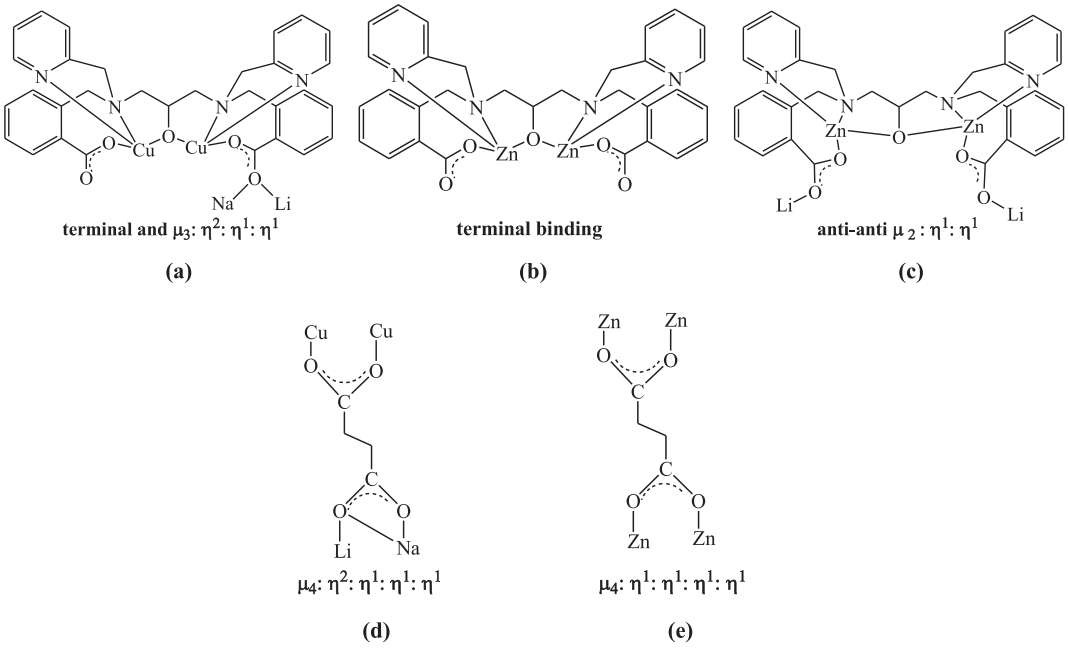

Chart 1. Observed coordination modes of the ligand $cpdp^{3-}$ (a, b, c) and succinate (d, e) in complexes **1** and **2**.

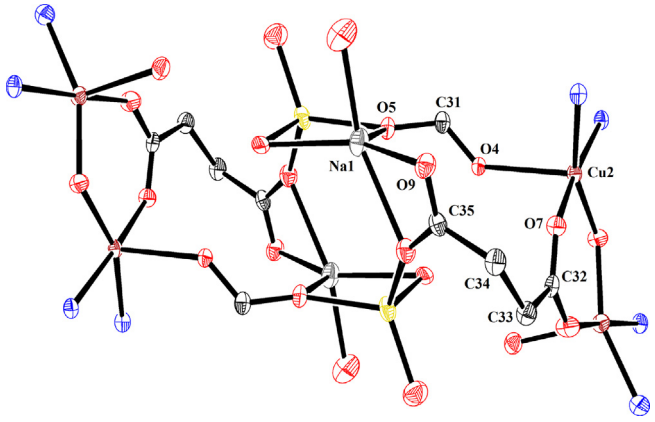

Fig. 2. Core framework of **1** showing metallomacrocyclic topologies.

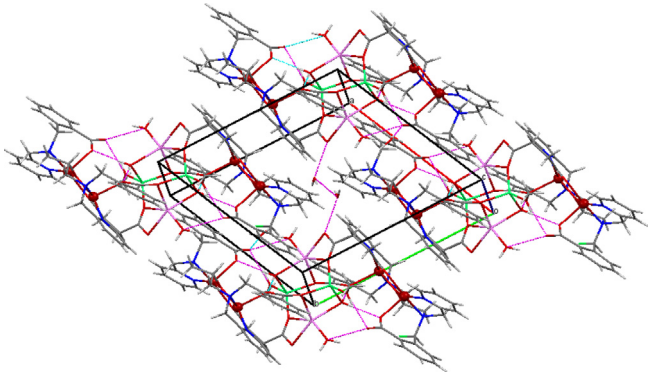

Fig. 3. Packing diagram of **1** showing hydrogen bonding interactions.

3.3. Description of the X-ray crystal structure of **2**

Complex **2** crystallized in the triclinic system and the structure was solved in $P\bar{1}$ space group. The asymmetric unit of crystal structure of **2** (Fig. S2, Supplementary Information) consists of one lithium(I), one sodium(I) and four zinc(II) ions, two $cpdp^{3-}$ and one succinate ligand, and two coordinated water molecules. The asymmetric unit also contains two chloride and three bromide ions as counter ions along with six methanol and nineteen water molecules as solvents of crystallization. The full structure is generated by growing the asymmetric unit through center of inversion. To balance the total charge, two protons have to be included in the structure. However, the protons could not be located precisely from Fourier density map. A view of the crystal structure of hetero-decanuclear unit of **2** is illustrated in Fig. 4. Formation of this hetero-decanuclear complex is accomplished by the self-assembly of two tetranuclear $[Zn_4(cpdp)_2(suc)]$ complexes and two $[Li(H_2O)_2]^+$ ions linked entirely by four carboxylate groups of $cpdp^{3-}$ ligands in a μ_2:η^1:η^1 *anti-anti* bidentate fashion (Chart 1). In essence, two $[Li(H_2O)_2]^+$ ions act as interconnectors between the two $[Zn_4(cpdp)_2(suc)]$ complexes. Consequently, a metallomacrocyclic ring demarcated by Li(1)–O(10)–C(62)–O(9)–Zn(4)–O(6)–Zn(3)–O(7)–C(48)–O(8)–Li(1′)–O(10′)–C(62′)–O(9′)–Zn(4′)–O(6′)–Zn(3′)–O(7′)–C(48′)–O(8′) is shaped through the symmetrical arrangement of two lithium and four zinc ions with four and five coordination environments, respectively (Fig. 5). The core of each tetranuclear $[Zn_4(cpdp)_2(suc)]$ species is constructed by two $[Zn_2(cpdp)]^+$ units bridged by a succinate group in a μ_4:η^1:η^1:η^1:η^1 mode (Chart 1). The two zinc centers within each $[Zn_2(cpdp)]^+$ unit are bridged and chelated by an alkoxide oxygen of $cpdp^{3-}$ ligand and a COO^- linkage of succinate. The solid state structure of **2** also consists of a 20-membered large size cavity of ~5.4 Å.

The eight zinc sites have identical coordination environments, with each site exhibiting a highly distorted trigonal bipyramidal geometry (τ = 0.672 for Zn1, τ = 0.828 for Zn2, τ = 0.814 for Zn3, and τ = 0.740 for Zn4) [44]. Each zinc center is surrounded by a bridging alkoxide oxygen, a terminal carboxylate oxygen, a tertiary amine nitrogen, a pyridine nitrogen from a $cpdp^{3-}$ ligand, and one bridging succinate oxygen. From the basal planes, the zinc ions are deviated by 0.190 (Zn1), 0.215 (Zn2), 0.200 (Zn3) and 0.185 Å (Zn4). The coordination environment of lithium(I) ion shows a distorted tetrahedral geometry, with two carboxylate oxygen and two

Please cite this article as: S. Haldar, N. Dutta, G. Vijaykumar et al., Synthesis, structure and properties of new heterometallic octanuclear $Li_2Na_2Cu_4$ and decanuclear Li_2Zn_8 complexes, Polyhedron, https://doi.org/10.1016/j.poly.2019.03.013

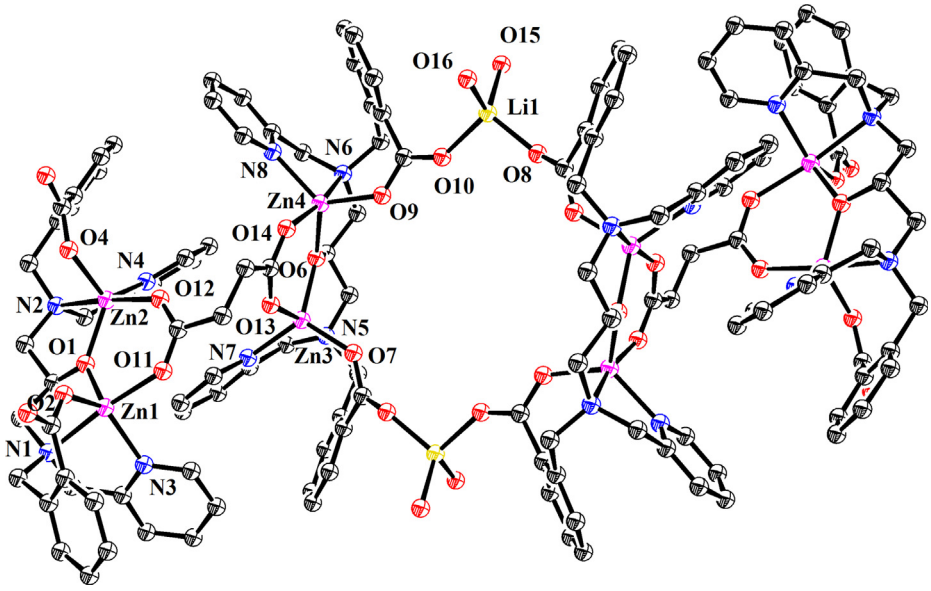

Fig. 4. X-ray crystal structure of **2** with atom numbering scheme. Hydrogen atoms are omitted for clarity.

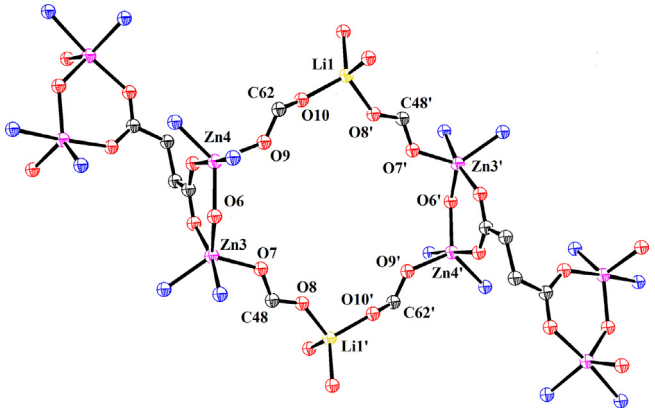

Fig. 5. Core framework of **2** showing a metallomacrocyclic ring.

water oxygen atoms. Again, the coordination environment of sodium(I) ion exhibits a highly distorted octahedral geometry completed by two carboxylate oxygen and four water oxygen atoms. The Zn–$O_{bridging\ alkoxide}$ bond distances [Zn1–O1, 1.950(4); Zn2–O1, 1.950(4), Zn3–O6, 1.962(4) and Zn4–O6, 1.946(3) Å] are within the range of those reported previously [26], and the values indicate that Zn–O alkoxide bridge is asymmetric. The Zn–$O_{bridging\ succinate}$ bond distances [Zn1–O11, 2.025(4); Zn2–O12, 2.047(4), Zn3–O13, 2.043(3); Zn4–O14, 2.023(4) Å] indicate that the Zn-O succinate bridge is also symmetric. Within each tetranuclear [Zn_4(cpdp)$_2$(suc)] complex, the average intra-dimeric Zn···Zn separation is 3.487 Å and the average inter-dimeric Zn···Zn separation is 6.839 Å. It may be significant to mention that the moderate intramolecular $\pi\cdots\pi$ stacking interactions have been observed within each tetranuclear species due to face-to-face sequential arrangement of benzoate-pyridyl-pyridyl-benzoate rings (Fig. S3, Supplementary Information). Close analysis of X-ray structure specifies such interactions between the adjacent benzoate-pyridyl, pyridyl-pyridyl, and pyridyl-benzoate rings, with average closest contacts of 4.026, 3.762, and 3.604 Å, respectively. **2** can also be viewed as a rare example of a hetero-decanuclear Li_2Zn_8 complex displaying three different binding modes of carboxylates (terminal, *anti-anti* μ_2:η^1:η^1 and μ_4:η^1:η^1:η^1:η^1). Crystal data and refinement parameters for **1** and **2** are summarized in Table S1. Selected bond lengths and angles are given in Table 1.

3.4. Spectroscopic studies

In the FTIR spectrum of **1**, the strong bands appearing at 1589, 1580 and 1563 cm^{-1}, and 1459, 1430 and 1403 cm^{-1} are assigned to the $\nu_{as}(COO^-)$ and $\nu_s(COO^-)$ vibrations of the carboxylates, respectively (Fig. S4, Supplementary Information). The relatively higher difference of Δ ($\Delta = \nu_{as}(COO^-) - \nu_s(COO^-)$) of ~186 cm^{-1} is ascribed to the monodentate terminal as well as monodentate bridging mode of carboxylate coordination [45,46]. The value of Δ at ~150 cm^{-1} frequently indicates the *syn-syn* bidentate bridging coordination of succinate [45,46]. The occurrence of *syn-anti* bidentate bridging mode of carboxylate and chelating binding mode of succinate is manifested by significantly lower value of Δ at ~104 cm^{-1} [45,46]. The FTIR spectrum of **2** exhibits the strong bands at 1595, 1588 and 1571 cm^{-1}, and 1447, 1430 and 1394 cm^{-1} which correspond to the $\nu_{as}(COO^-)$ and $\nu_s(COO^-)$ vibrations of the carboxylates, respectively (Fig. S5, Supplementary Information). The monodentate terminal coordination of carboxylate group is indicated by the relatively higher difference of Δ at ~201 cm^{-1}. The comparatively lower values of Δ at ~158 and 124 cm^{-1} specify the existence of *syn-syn* bidentate bridging mode of succinate and *anti-anti* bidentate bridging mode of carboxylate, respectively [45,46]. In addition, the strong bands at 1609 (**1**) and 1608 (**2**) cm^{-1} are indicative of ν(C=N) stretching vibrations of pyridyl functionality of the ligand backbone.

We have carried out electronic absorption spectroscopy of both **1** and **2** by recording their spectra (Fig. S6, Supplementary Information) in methanol solution in the range of 200–900 nm. Broad absorption band with maxima at 693 nm (ε, 460 M^{-1} cm^{-1}) for **1**, corresponds to the d-d transition. The intense absorption bands at 259 nm (ε, 64956 M^{-1} cm^{-1}) for **1**, and 264 nm (ε, 50518 M^{-1} cm^{-1}) for **2** are observed, due to the metal ion-bound ligand-based charge transfer transitions.

The ^{1}H NMR spectrum complex **2** shows a triplet at 3.09 ppm for eight hydrogens of succinate and a broad multiplet in the range of 3.12–4.24 ppm for fifty two –CH_2– protons of the ligands. The presence of sixty four aromatic protons has been exhibited by broad multiplets in the range of 6.72–7.64 ppm. In the ^{13}C NMR

Please cite this article as: S. Haldar, N. Dutta, G. Vijaykumar et al., Synthesis, structure and properties of new heterometallic octanuclear $Li_2Na_2Cu_4$ and decanuclear Li_2Zn_8 complexes, Polyhedron, https://doi.org/10.1016/j.poly.2019.03.013

Table 1
Selected bond distances (Å) and angles (°) for $[Li_2Na_2Cu_4(cpdp)_2(suc)_2(CH_3OH)_2(H_2O)_4]Cl_2{\cdot}6H_2O$ (**1**) and $Na(H_3O)_2[Li_2Zn_8(cpdp)_4(suc)_2(H_2O)_4]Cl_2Br_3{\cdot}6MeOH{\cdot}19H_2O$ (**2**).

Bond distances [Å]	
1	**2**
Cu(1)–O(1) 1.896(3)	Zn(1)–O(1) 1.950(4)
Cu(1)–O(6) 1.931(3)	Zn(1)–O(2) 1.987(4)
Cu(1)–N(3) 1.986(4)	Zn(1)–O(11) 2.025(4)
Cu(1)–N(1) 2.033(4)	Zn(1)–N(1) 2.222(4)
Cu(1)–O(2) 2.214(3)	Zn(1)–N(3) 2.054(4)
Cu(2)– O(1) 1.896(3)	Zn(2)–O(1) 1.949(4)
Cu(2)–O(7) 1.962(3)	Zn(2)–O(4) 1.985(4)
Cu(2)–N(4) 1.982(4)	Zn(2)–O(12) 2.048(4)
Cu(2)–N(2) 2.042(4)	Zn(2)–N(2) 2.214(4)
Cu(2)–O(4) 2.192(3)	Zn(2)–N(4) 2.047(4)
Li(1)–O(5) 1.956(9)	Zn(3)–O(6) 1.962(3)
Li(1)–O(2 W) 2.012(9)	Zn(3)–O(7) 1.981(4)
Li(1)–O(10) 1.899(10)	Zn(3)–O(13) 2.043(3)
Li(1)–O(8) 1.904(9)	Zn(3)–N(5) 2.203(4)
Na(1)–O(8) 2.506(4)	Zn(3)–N(7) 2.065(4)
Na(1)–O(9) 2.314(4)	Zn(4)–O(6) 1.945(3)
Na(1)–O(2 W) 2.308(4)	Zn(4)–O(9) 1.976(4)
Na(1)–O(1 W) 2.318(5)	Zn(4)–O(14) 2.023(4)
Na(1)–O(5) 2.307(4)	Zn(4)–N(6) 2.215(4)
	Zn(4)–N(8) 2.074(5)
	Li(1)–O(8) 1.892(10)
	Li(1)–O(16) 1.879(11)
	Li(1)–O(10) 1.936(11)
	Li(1)–O(15) 1.941(10)
Bond angles [°]	
1	**2**
O(1)–Cu(1)–O(6) 96.66(14)	O(1)–Zn(1)–O(2) 107.65(15)
O(1)–Cu(1)–N(3) 157.44(16)	O(1)–Zn(1)–O(11) 98.17(14)
O(6)–Cu(1)–N(3) 91.88(15)	O(1)–Zn(1)–N(1) 83.05(15)
O(1)–Cu(1)–N(1) 85.99(15)	O(1)–Zn(1)–N(3) 117.13(16)
O(6)–Cu(1)–N(1) 174.85(15)	O(2)–Zn(1)–O(11) 95.64(15)
N(3)–Cu(1)–N(1) 84.08(16)	O(2)–Zn(1)–N(1) 90.71(16)
O(1)–Cu(1)–O(2) 97.84(14)	O(2)–Zn(1)–N(3) 132.44(16)
O(6)–Cu(1)–O(2) 92.13(14)	O(11)–Zn(1)–N(1) 172.81(16)
N(3)–Cu(1)–O(2) 102.67(15)	O(11)–Zn(1)–N(3) 93.22(17)
N(1)–Cu(1)–O(2) 91.87(14)	N(3)–Zn(1)–N(1) 79.98(17)
O(1)–Cu(2)–O(7) 96.48(13)	O(1)–Zn(2)–O(4) 116.07(16)
O(1)–Cu(2)–N(4) 160.68(15)	O(1)–Zn(2)–O(12) 97.48(15)
O(7)–Cu(2)–N(4) 93.01(14)	O(1)–Zn(2)–N(2) 81.23(15)
O(1)–Cu(2)–N(2) 85.23(14)	O(1)–Zn(2)–N(4) 123.10(17)
O(7)–Cu(2)–N(2) 173.00(14)	O(4)–Zn(2)–O(12) 95.02(16)
N(4)–Cu(2)–N(2) 83.44(15)	O(4)–Zn(2)–N(2) 91.91(17)
O(1)–Cu(2)–O(4) 99.17(13)	O(4)–Zn(2)–N(4) 117.40(17)
O(7)–Cu(2)–O(4) 94.40(12)	O(12)–Zn(2)–N(2) 172.78(16)
N(4)–Cu(2)–O(4) 96.83(14)	N(4)–Zn(2)–O(12) 95.96(16)
N(2)–Cu(2)–O(4) 92.01(13)	N(4)–Zn(2)–N(2) 79.00(16)
Li(1)–O(5)–Na(1) 89.0(3)	O(6)– Zn(3)–O(7) 114.06(16)
Li(1)–O(8)–Na91) 112.6(3)	O(6)–Zn(3)–O(13) 98.78(14)
O(5)–Na(1)–O(2 W) 82.01(13)	O(6)–Zn(3)–N(5) 81.83(15)
O(5)–Na(1)–O(9) 128.98(14)	O(6)–Zn(3)–N(7) 124.99(15)
O(2 W)–Na(1)–O(9) 147.30(15)	O(7)–Zn(3)–O(13) 93.39(15)
O(5)–Na(1)–O(1 W) 100.43(15)	O(7)–Zn(3)–N(5) 91.93(16)
	O(7)–Zn(3)–N(7) 117.96(16)
	O(13)–Zn(3)–N(5) 173.85(15)
	O(13)–Zn(3)–N(7) 94.89(15)
	N(7)–Zn(3)–N(5) 79.87(16)
	O(6)–Zn(4)–O(9) 112.92(16)
	O(6)–Zn(4)–O(14) 96.98(15)
	O(6)–Zn(4)–N(6) 82.23(15)
	O(6)–Zn(4)–N(8) 119.94(17)
	O(9)–Zn(4)–O(14) 97.95(18)
	O(9)–Zn(4)– N(6) 92.44(17)
	O(9)–Zn(4)–N(8) 124.58(17)
	O(14)–Zn(4)–N(6) 168.98(19)
	O(14)–Zn(4)–N(8) 91.33(19)
	N(8)–Zn(4)–N(6) 79.70(17)

spectrum of complex **2** (Fig. S7, Supplementary Information), characteristic peaks at 176.11, 176.22, 180.70 and 180.91 ppm are observed due to the presence of one type of monodentate terminal carboxylate of $cpdp^{3-}$ ligand, one type of bidentate bridging carboxylate of $cpdp^{3-}$ ligand and two similar bidentate bridging succinate carboxylates but under different dimetallic coordination environments, respectively. The ^{13}C NMR signals appeared in the range of 51.81–63.72 ppm and 122.88–157.57 ppm, correspond to the aliphatic and aromatic carbons, respectively.

3.5. Thermal property and stability

Thermogravimetric analysis (TGA) of **1** (Fig. 6) shows an initial weight loss of 5.46% (calcd: 5.50%) in the temperature range of 97–180 °C corresponding to the loss of six lattice waters. Subsequently, the second weight loss of 7.45% (calcd: 7.40%) from 251 to 280 °C and the third weight loss of 17.90% (calcd: 18.00%) from 281 to 443 °C could be attributed to the losses of four coordinated water and two coordinated methanol molecules, and eight CO_2 molecules, respectively. Further decomposition of metal–organic framework is observed between 479 and 811 °C, resulting in the formation of Li_2O, Na_2O and CuO as possible final residues. The TGA plot of **2** (Fig. 6) exhibits the first weight loss of 9.65% (calcd: 9.69%) in the temperature range of 30–101 °C indicating the loss of twenty one lattice waters. The second weight loss of 4.88% (calcd: 4.92%) in the temperature range of 257–287 °C shows the removal of six uncoordinated methanol molecules. The third and fourth weight losses of 1.82% (calcd: 1.84%) from 305 to 317 °C and 15.28% (calcd: 15.37%) from 324 to 420 °C correspond to the losses of four coordinated water molecules, and twelve CO_2 molecules, respectively. Then, the metal–organic framework undergoes decomposition between 472 and 745 °C, giving rise to Li_2O, Na_2O and ZnO as possible final residues

We have performed the PXRD experiment with Bragg angular range, *i.e.*, 2θ ($5° < 2\theta < 90°$) at room temperature for both complexes **1** and **2** using the microcrystalline samples obtained upon drying the crystals in the vacuum desicator. Then we have heated both these microcrystalline samples at ~100 and 180 °C and again performed their PXRD measurement. The patterns of PXRD spectra (Figs. S8 & S9, Supplementary Information) obtained for **1** and **2** before and after heating the samples, are more or less same without any significant change. Additionally, no characteristic new peaks are observed within the limits of experiment, suggesting that the structures are thermally stable up to a certain temperature. However, for both **1** and **2**, there are minor changes of the intensity of the peaks before and after heating the samples. There is hardly any shift of the peaks in the spectra obtained before and after heating the samples. This results also indicate that upon the

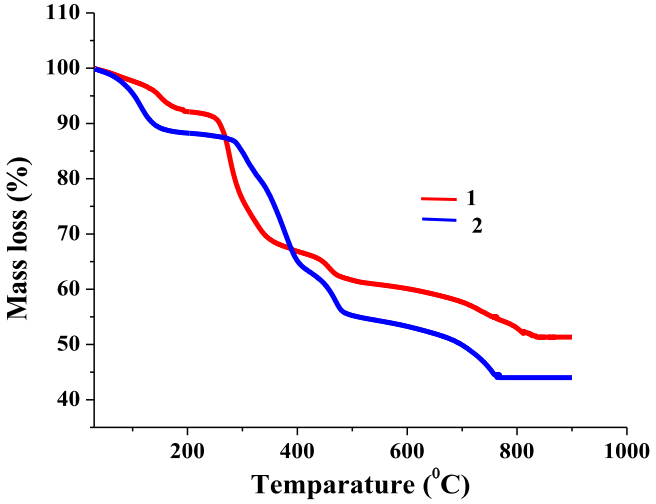

Fig. 6. TGA plot of **1** and **2** under N_2 gas atmosphere at heating rate of 10 °C min^{-1}.

Please cite this article as: S. Haldar, N. Dutta, G. Vijaykumar et al., Synthesis, structure and properties of new heterometallic octanuclear $Li_2Na_2Cu_4$ and decanuclear Li_2Zn_8 complexes, Polyhedron, https://doi.org/10.1016/j.poly.2019.03.013

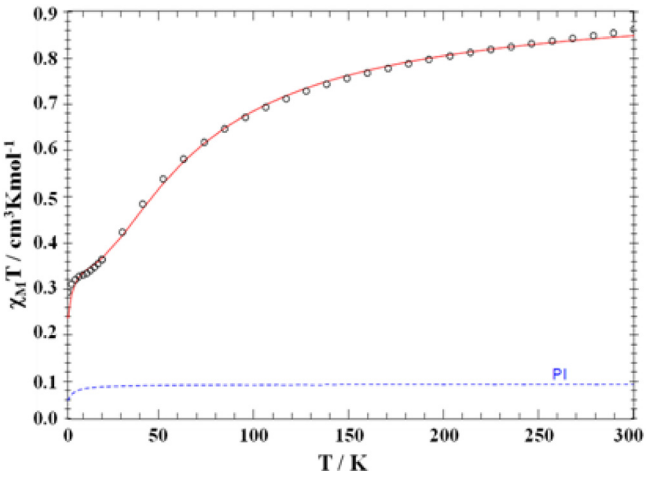

Fig. 7. Temperature dependence of $\chi_M T$ for **1**. The red solid line corresponds to the best fit obtained with the isotropic exchange Hamilton described in the text.

loss of lattice waters from complexes **1** and **2**, their structures are retained.

3.6. Magnetic properties

Variable temperature magnetic susceptibility data were collected for **1** in a temperature range of 2–300 K under an applied field of 1 Tesla on powdered microcrystalline sample with a SQUID magnetometer (MPMS-7, Quantum Design, Fig. 7). For the interpretation of the magnetic data, only the asymmetric unit was taken into account. At room temperature a χ_MT-value of 0.85 $cm^3\,Kmol^{-1}$, which is very close to the expected value of 0.75 $cm^3\,Kmol^{-1}$ for two uncoupled spins with $S_1 = S_2 = {}^1/_2$. By lowering the temperature up to 100 K, a gradual decrease in χ_MT value is documented. Further cooling results in a sharp decrease reaching to a value of 0.32 $cm^3\,Kmol^{-1}$ at 2 K. This reflects the fact that the magnetic behavior of the title complex is determined by moderate antiferromagnetic interactions within the molecule. The coupling within this complex can be described by the simplest possible Heisenberg Spin Hamiltonian multiplied by 2 in order to account for the two [Cu_2] dimers: $H = 2 \times [-2JS_1S_2]$. This is because the coupling between the [Cu_2] dimers is expected to be negligible in front of the moderate antiferromagnetism observed within the intradimers. Indeed, the copper(II) ions of different pairs which are separated by 10.839 Å are connected only by the alkali metal ions bridged by succinate and carboxylate moieties at the two ends. A good fit of the data can be obtained by including the weakly coupled paramagnetic impurities. The magnetic data can be simulated in adequate manner with $J = -22.03\ cm^{-1}$ and $g_1 = g_2 = 2.05$. A TIP of $400 \times 10^{-6}\ cm^3\,Kmol^{-1}$ was included while simulating the magnetic data.

4. Conclusion

In conclusion, complexation of copper(II) and zinc(II) ions with H_3cpdp and succinate ligands led to the isolation of two unprecedented metallomacrocyclic octanuclear [$Li_2Na_2Cu_4$] (**1**) and decanuclear [Li_2Zn_8] (**2**) complexes. Both **1** and **2** represent the first examples of succinate-bridged heterometallic high nuclearity complexes ($N \geq 6$) with any class of bridging or non-bridging ligand. Complexes **1** and **2** display several versatile coordination-cum-binding modes of the carboxylate and succinate groups studied by X-ray crystallography and FTIR. Among these, tridentate μ_3:η^2:η^1:η^1 bridging mode of carboxylate and μ_4:η^2:η^1:η^1:η^1 bridging mode of succinate in **1**, and *anti-anti* μ_2:η^1:η^1 bidentate bridging mode of carboxylate and μ_4:η^1:η^1:η^1:η^1 bridging mode of succinate in **2** are quite sporadic. The presence of Li/Na ions and μ_4:η^2:η^1:η^1:η^1/μ_4:η^1:η^1:η^1:η^1 bridging mode of succinate appears to provide the stabilizing factors for the heterometallic octanuclear [$Li_2Na_2Cu_4$] and decanuclear [Li_2Zn_8] cores. Variable temperature magnetic studies of **1** show antiferromagnetic interactions among the copper centers with $J = -22.03\ cm^{-1}$. This work not only offers an outlook towards the development of new heterometallic multinuclear complexes, but also suggests the potential for advancing new classes of multifunctional materials by using multinuclear transition metal complexes. Currently, we are pursuing our research work to prepare different heterometallic multinuclear complexes of other 3d transition metals based on these unique coordination-cum-bridging abilities of succinate as well as glutarate/adipate ions supported by the polydentate ligand, H_3cpdp.

Acknowledgements

The work was strongly supported by The Council of Scientific & Industrial Research (CSIR) (Grant No.: 01(2732)/13/EMR-II), New Delhi. The DST-FIST and UGC-SAP programs are acknowledged for providing the instrumental facilities in the Department of Chemistry, University of Kalyani. The Contingency Grant provided by the DST-PURSE program in the Department of Chemistry is also acknowledged. S.H. greatly acknowledges the RGNF received from UGC, New Delhi.

Appendix A. Supplementary data

CCDC 1860696 and 1860697 contains the supplementary crystallographic data for complexes **1** and **2**. These data can be obtained free of charge via http://www.ccdc.cam.ac.uk/conts/retrieving.html, or from the Cambridge Crystallographic Data Centre, 12 Union Road, Cambridge CB2 1EZ, UK; fax: (+44) 1223-336-033; or e-mail: deposit@ccdc.cam.ac.uk. Supplementary data to this article can be found online at https://doi.org/10.1016/j.poly.2019.03.013.

References

[1] V. Chandrasekhar, D. Sahoo, R.S. Narayanan, R.J. Butcher, F. Lloret, E. Pardo, Dalton Trans. 42 (2013) 8192.
[2] A.A. Dar, S. Sen, S.K. Gupta, G.N. Patwari, R. Murugavel, Inorg. Chem. 54 (2015) 9458.
[3] C.H. Chiang, Y.W. Tzeng, C.I. Yang, M. Nakano, W.L. Wan, L.L. Lai, G.H. Leed, Dalton Trans. 46 (2017) 1237.
[4] T.R. Zheng, L.L. Qian, M. Li, Z.X. Wang, K. Li, Y.Q. Zhang, L. Li, Bao Bing Wu, Dalton Trans. 47 (2018) 9103.
[5] J.J. Henkelis, L.F. Jones, M.P. De, C.A. Miranda, H.M.A. Kilner, Inorg. Chem. 49 (2010) 11127.
[6] E.C. Constable, C.E. Housecroft, J.A. Zampese, G. Zhang, Polyhedron 44 (2012) 150.
[7] H. Zhang, Jin Zhang, Y. Rui Liu, W. Li, W Li Liu, Eur. J. Inorg. Chem. (2016) 4134.
[8] T. Glaser, Chem. Commun. 47 (2011) 116.
[9] S.A. Corrales, J.M. Cain, K.A. Uhlig, A.M. Mowson, C. Papatriantafyllopoulou, M. K. Peprah, A. Ozarowski, A.J. Tasiopoulos, G. Christou, M.W. Meisel, C. Lampropoulos, Inorg. Chem. 55 (2016) 1367.
[10] T. Jenkins, A.M. Garnero, S.A. Corrales, E.R. Williams, A.M. Mowson, A. Ozarowski, W. Wernsdorfer, G. Christou, C. Lampropoulos, Inorg. Chem. 56 (2017) 14755.
[11] M. Charalambous, Eleni E. Moushi, T.N. Nguyen, A.M. Mowson, G. Christou, A,, J., Tasiopoulos,, Eur. J. Inorg. Chem. (2018) 3905.
[12] Y.Z. Zheng, E.M. Pineda, M. Helliwell, R.E.P. Winpenny, Chem. Eur. J. 18 (2012) 4161.
[13] A.M. Ako, I.J. Hewitt, V. Mereacre, R. Clrac, W. Wernsdorfer, C.E. Anson, A.K. Powell, Angew. Chem. 118 (2006) 5048, Angew. Chem., Int. Ed. 45 (2006) 4926-4929.
[14] C.J. Milios, A. Vinslava, W. Wernsdorfer, S. Moggach, S. Parsons, S.P. Perlepes, G. Christou, E.K. Brechin, J. Am. Chem. Soc. 129 (2007) 2754.
[15] D.A. Whittington, S.J. Lippard, J. Am. Chem. Soc. 123 (2001) 827.
[16] C. Gerdemann, C. Eicken, B. Krebs, Acc. Chem. Res. 35 (2002) 183.

Please cite this article as: S. Haldar, N. Dutta, G. Vijaykumar et al., Synthesis, structure and properties of new heterometallic octanuclear $Li_2Na_2Cu_4$ and decanuclear Li_2Zn_8 complexes, Polyhedron, https://doi.org/10.1016/j.poly.2019.03.013

[17] C.E. Elwell, N.L. Gagnon, B.D. Neisen, D. Dhar, A.D. Spaeth, G.M. Yee, W.B. Tolman, Chem. Rev. 117 (2017) 2059.
[18] E.I. Solomon, D.E. Heppner, E.M. Johnston, J.W. Ginsbach, J. Cirera, M. Qayyum, E.M.T. Kieber, C.H. Kjaergaard, R.G. Hadt, Li., Tian,, Chem. Rev. 114 (2014) 3659.
[19] A. Patra, S.K. Saha, T.K. Sen, L. Carrella, G.T. Musie, A.R. Khuda-Bukhsh, M. Bera, Eur. J. Inorg. Chem. (2014) 5217.
[20] Z. Chen, Y. Shen, L. Li, H. Zou, X. Fu, Z. Liu, K. Wang, F. Liang, Dalton Trans. 46 (2017) 15032.
[21] D. Ghoshal, T.K. Maji, S.G. Mostafa, T.H. Sain, J. Lu, E. Zangrando, J. Ribas, N.R. Chaudhuri, Dalton Trans. (2004) 1687.
[22] D.F. Li, Z. Liao, Y. Wei, F. Du, M. Wang, W. Chen, W. Li, X. Mao, Dalton Trans. (2003) 2164.
[23] A.K. Ghosh, D. Ghoshal, E. Zangrando, J. Ribas, N.R. Chaudhuri, Inorg. Chem. 46 (2007) 3057.
[24] P.M. Forster, A.K. Cheetham, Angew. Chem., Int. Ed. 41 (2006) 457.
[25] J.P. Costes, J.P. Laurent, J.M.M. Sanchez, J.S. Varela, M. Ahlgren, M. Sundberg, Inorg. Chem. 36 (1997) 4641.
[26] S. Haldar, G. Vijaykumar, L. Carrella, S. Batha, G.T. Musie, M. Bera, ACS Omega 2 (2017) 1535.
[27] M. Bera, G.T. Musie, D.R. Powell, Inorg. Chem. 48 (2009) 4625.
[28] S. Haldar, G. Vijaykumar, L. Carrella, G.T. Musie, M. Bera, New J. Chem. 42 (2018) 1276.
[29] R.L. Carlin, Magnetochemistry, Springer-Verlag, New York, 1986.
[30] N.F. Chilton, R.P. Anderson, L.D. Turner, A. Soncini, K.S. Murray, PHI, J. Comput. Chem. 34 (2013) 1164.
[31] A. Patra, S. Haldar, G. Vijaykumar, L. Carrella, A.K. Ghosh, M. Bera, Inorg. Chim. Acta 436 (2015) 195.
[32] Data Collection, SMART Software Reference Manual, Bruker-AXS, Madison, WI, 1998.
[33] Data Reduction, SAINT Software Reference Manual, Bruker-AXS, Madison, WI, 1998.
[34] G.M. Sheldrick, SADABS, University of Göttingen, Germany, Program for Multi-Scan Absorption Correction of Area Detector Data, 2002.
[35] C. Giacovazzo, A. Guagliardi, A.G.G. Moliterni, G. Polidori, R. Spagna, J. Appl. Crystallogr. 32 (1999) 115.
[36] (a) G. M. Sheldrick, SHELXL. Version 6.10 Reference Manual. Bruker-AXS, Madison, WI, 2000; (b) International Tables for Crystallography, Vol C, Tables 6.1.1.4, 4.2.6.8, and 4.2.4.2, Kluwer: Boston, 1995.
[37] G.M. Sheldrick, Crystal structure refinement with SHELXL, Acta Cryst. C 71 (2015) 3.
[38] O.V. Dolomanov, L.J. Bourhis, R.J. Gildea, J.A.K. Howard, H. Puschmann, OLEX2: a complete structure solution, refinement and analysis program, J. Appl. Cryst. 42 (2009) 339.
[39] S. Haldar, G. Vijaykumar, A.K. Ghosh, L. Carrella, M. Bera, Polyhedron 121 (2017) 130.
[40] N. Dutta, S. Haldar, G. Vijaykumar, S. Paul, A.P. Chattopadhyay, L. Carrella, M. Bera, Inorg. Chem. 57 (2018) 10802.
[41] A. Patra, T.K. Sen, A. Ghorai, G.T. Musie, S.K. Mandal, U. Ghosh, M. Bera, Inorg. Chem. 52 (2013) 2880.
[42] R.L. Rardin, W.B. Tolman, S.J. Lippard, New J. Chem. 15 (1991) 417.
[43] N. Scales, Y. Zhang, M. Bhadbhade, I. Karatchevtseva, L. Kong, G.R. Lumpkin, F. Li, Polyhedron 102 (2015) 130.
[44] A. Addison, T.N. Rao, J. Reedijk, J. van Rijn, G.C. Verschoor, J. Chem. Soc., Dalton Trans. (1984) 1349.
[45] G.B. Deacon, R.J. Phillips, Coord. Chem. Rev. 33 (1980) 227.
[46] K. Nakamoto, Infrared and Raman Spectra of Inorganic and Coordination Compounds, 4th ed., Wiley, New York, 1986, pp 231-233, 251, 253.

Please cite this article as: S. Haldar, N. Dutta, G. Vijaykumar et al., Synthesis, structure and properties of new heterometallic octanuclear $Li_2Na_2Cu_4$ and decanuclear Li_2Zn_8 complexes, Polyhedron, https://doi.org/10.1016/j.poly.2019.03.013